

Microwave-Driven Zeolite–Guest Systems Show Athermal Effects from Nonequilibrium Molecular Dynamics

Cristian Blanco[†] and Scott M. Auerbach^{*,†,‡}

Chemistry Department and Chemical Engineering Department, University of Massachusetts, Amherst, Massachusetts 01003

Received December 20, 2001

Over the past few years, a flurry of interest has emerged in using microwaves (MW) in chemical processes, such as catalyst synthesis, reactions, and separations.¹ For example, Turner et al.² have recently studied the effects of MW heating on a binary mixture, methanol/cyclohexane, adsorbed in siliceous zeolites FAU and MFI. They found that the effect on sorption selectivity from conventional heating can be reversed by applying MW radiation. However, because the MW period is long compared to typical thermalization time scales, it is not clear what microscopic energy distributions are responsible for the reversed selectivities discussed above. In the present communication, we focus on determining energy distributions in MW-driven zeolite–guest systems from microscopic simulations.

We studied industrially important zeolites that represent extremes of high charge (NaY) and low charge (de-aluminated Y (DAY) and silicalite) materials. We also studied guest molecules that represent extremes of polar (methanol) and nonpolar (benzene) species. We performed equilibrium molecular dynamics (MD) and nonequilibrium MD (NEMD) simulations on bare zeolites, and on zeolite–guest systems with single-component guest phases as well as with binary mixtures of guests. Molecular mechanics parameters to model zeolite framework vibrations were taken from the force field recently developed and validated by Jaramillo and Auerbach.³ Guest molecules were described by using harmonic potentials for bond, angle, and torsional motions, whereas Lennard-Jones potentials were used to represent host–guest and guest–guest nonbonding interactions. Long-range interactions were evaluated by using Ewald summations assuming fixed, partial charges on each particle, obtained either from the literature⁴ or from quantum chemical calculations.⁵ The fixed point charge approximation is reasonable because of the large frequency mismatch between the MW frequency and the frequency associated with electronic polarizabilities of oxide materials. To test the validity of our potential function, we compared simulated heats of sorption, dipole moments, diffusion constants, and vibrational spectra to those obtained experimentally, generally finding good agreement.⁶

In addition to equilibrium MD in the microcanonical (NVE) ensemble, which conserves total energy, we developed and applied an NEMD algorithm within the program Dizzy.⁷ The latter was obtained by modifying Newton's equations of motion to account for the external field, according to:

$$\begin{aligned}\dot{\vec{r}}_i(t) &= \vec{p}_i(t)/m_i \\ \dot{\vec{p}}_i(t) &= \vec{F}_i(t) + q_i \vec{E}(t)\end{aligned}\quad (1)$$

where (m_i , q_i , \vec{r}_i , \vec{p}_i) are the mass, charge, position, and momentum

of particle i . In eq 1, \vec{F}_i is the force on the i th particle in the absence of the external field, and $\vec{E}(t)$ is the MW electric field, which is assumed to be spatially independent and temporally monochromatic according to: $\vec{E}(t) = \vec{z} \cdot E \cdot \cos \omega t$. In our simulations, we have set $\omega = 9.4 \times 10^{11}$ Hz, which is at the blue end of the MW spectrum. In future work, we will test the effect of using other MW frequencies.

To compare with experiments with steady-state temperatures, which are produced by using carrier gases such as He,^{2,8} we introduced a thermostat to simulate the cooling that occurs when carrier gas particles collide with MW heated zeolite–guest particles on the inflow side. In all the simulations reported here, all zeolite and guest atoms evolve dynamically and are treated consistently by the thermostat. We initially used the Nosé–Hoover chain approach,⁹ varying the thermostat parameters over a wide range. We observed two regimes: for low thermostat frequencies the simulations exhibit runaway heating, while for high frequencies no MW heating is observed. We found no intermediate regime, possibly because the Nosé–Hoover approach influences all atoms at each step. We then applied Andersen's stochastic velocity-replacement method,¹⁰ which allows us to control the number of particles influenced at each velocity replacement. This approach yielded steady states that are reasonably robust to changes in thermostat parameters. For most of the simulations reported here, we found that replacing the 3d velocity of one atom every 10 fs (on average) gives robust steady states. This corresponds to replacing all velocities every 7 ps (on average). While stochastic velocity-replacement likely reflects the microscopic dynamics of cooling in this system, the final steady states we obtain do depend on the nature of the thermostat. To explore this issue more fully, we plan in future work to consider other thermostats, explicit He collisions, and the relevant energy balances between system and thermostat.

To explore how changing the system influences MW heating properties, we define a time-dependent system temperature, $\langle T(t) \rangle$, obtained by properly normalizing the total system kinetic energy at each MD time step. This can be calculated with or without the perturbations of the field and the thermostat. To distinguish between energy distributions in equilibrium systems from those in MW-driven, steady-state systems, we also define steady-state temperatures for each atom type in the system, denoted $T_{ss}(i)$, where i labels the atom type. These were obtained by exploiting the fact that, even in the NEMD simulations, all velocity distributions remained Gaussian. We thus extracted effective temperatures for each atom type from the second moment of these distributions. A system was deemed to be thermal when all atom types have the same temperature within statistical precision; athermal systems are those where different atom types exhibit statistically different temperatures.

In Figure 1 we show the time-dependent temperature, $\langle T(t) \rangle$, for the three different zeolites under various field strengths, in all cases without the thermostat. We observe that two distinct heating regimes

* Corresponding author. E-mail: auerbach@chem.umass.edu.

[†] Chemistry Department.

[‡] Chemical Engineering Department.

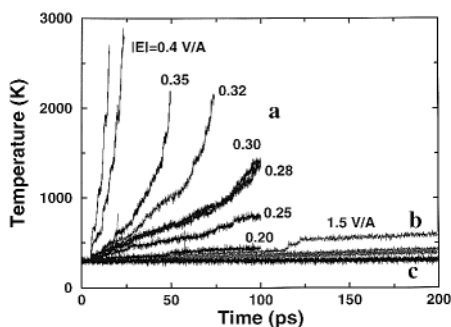


Figure 1. Heating of bare zeolites with different MW strengths. External field frequency 9.4×10^{11} Hz: (a) NaY; (b) silicalite; and (c) siliceous-Y.

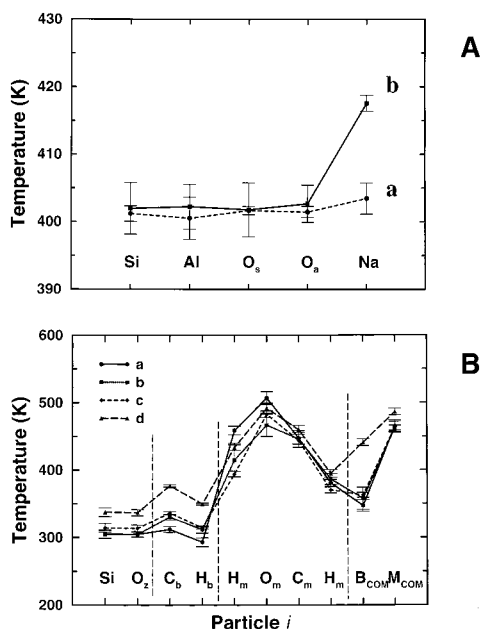


Figure 2. (A) Energy distributions in NaY at (a) thermal equilibrium (400 K) and (b) nonequilibrium, with external field strength $|E| = 0.30$ V/Å, and thermostat period $\Delta t = 10$ fs/particle. (B) Steady-state energy distributions for binary mixtures in siliceous-Y (a) and 1:1 (b), 2:2 (c), 4:4, and (d) 8:8 methanol-benzene per unit cell. The regions in the graph represent (from left to right) zeolite, benzene atoms, methanol atoms, and centers-of-mass of benzene and methanol, respectively.

can be identified: linear heating for weak fields and exponential heating for strong fields. The former is characteristic of siliceous zeolites over a large range of external field strengths. The presence of Na cations in Na-Y zeolite (Si:Al = 2) produces strong coupling with the external field, due mainly to the higher mobility of the ions compared with that of the framework atoms, which allows larger fluctuations of the instantaneous dipole moment distributed throughout the zeolite. This is consistent with the runaway conditions observed experimentally when applying MWs to zeolites without using a carrier gas.¹¹

With no MW field we simulate equilibrium states, whereas with both MWs and the thermostat we simulate steady states. Here we address the question of whether such systems, with both equilibrium and steady-state temperatures, have qualitatively similar energy distributions. These energy distributions are shown in Figure 2A for NaY at ca. 400 K. At equilibrium, all atoms in the system are at the same temperature, as expected. In contrast, when Na-Y zeolite is exposed to MW energy, the effective steady-state temperature of Na atoms is considerably higher than that for the rest of the framework, indicating an athermal energy distribution. This athermal effect arises because, even though the Na ions

continuously dissipate energy into the framework, the dissipation is not efficient enough in our simulations to completely thermalize the absorbed energy. In future work, we will study the sensitivity of energy transfer rates to the parameters in our model.

In other simulations, on methanol in both of the siliceous zeolites (data not shown), we have found that steady-state host-guest systems can be maintained with different temperatures for the host and the guest. This can also be rationalized based on inefficient energy transfer between host and methanol guest molecules. We will detail these results in a forthcoming publication. However, a binary mixture might be expected to exhibit efficient energy transfer between the guests, suggesting that it might be unlikely to maintain different guests at different steady-state temperatures.

To address this question, we have modeled different loadings of a methanol-benzene binary mixture in both siliceous zeolites. Figure 2B shows the effective steady-state temperatures for each particle type, when different amounts of equimolar mixtures of methanol-benzene are adsorbed in siliceous-Y zeolite. Even under these conditions, we found statistically different temperatures for each component, where $T_{\text{methanol}} \gg T_{\text{benzene}} > T_{\text{zeolite}}$. This remarkable result suggests that methanol dissipates energy to benzene, though much too slowly to approach thermal equilibrium while under steady-state conditions.

We thus conclude that MW heating of binary mixtures in zeolites can indeed produce energy distributions that are qualitatively different from those obtained with conventional heating. Heating an equilibrium binary mixture of methanol-cyclohexane in siliceous-Y would desorb more cyclohexane because of its higher heat of adsorption. However, MW heating the same system, leading to the energy distribution in Figure 2B, would desorb more methanol because of its higher dipole moment. In future work, we will address whether such athermal conditions and reversed desorption selectivities persist for mixtures flowing through zeolite membranes.

Acknowledgment. We acknowledge support from the NSF (Career, CTS-9734153), a Sloan Research Fellowship (BR-3844), and a Camille Dreyfus Teacher-Scholar Award (TC-99-041).

References

- (1) (a) Mingos, D. P.; Baghurst, D. R. *Chem. Soc. Rev.* **1991**, *20*, 1-47. (b) Galema, S. A. *Chem. Soc. Rev.* **1997**, *26*, 233-238. (c) Cundy, C. S.; Plaisted, R. J.; Zhao, J. P. *Chem. Commun.* **1998**, 1465-1466. (d) Rao, K. J.; Vaidyanathan, B.; Ganguli, M.; Ramakrishnan, P. A. *Chem. Mater.* **1999**, *11*, 882-895. (e) Girmus, I.; Jancke, K.; Vetter, R.; Richter-Mendau, J.; Caro, J. *Zeolites* **1995**, *15*, 33-39.
- (2) Turner, M. D.; Laurence, R. L.; Conner, W. C.; Yngvesson, K. S. *AIChE J.* **2000**, *46*, 758-768.
- (3) Jaramillo, E.; Auerbach, S. M. *J. Phys. Chem. B* **1999**, *103*, 9589-9594.
- (4) (a) Gale, J. D.; Catlow, C. R. A.; Carruthers, J. R. *Chem. Phys. Lett.* **1993**, *216*, 155-161. (b) Shah, R.; Gale, J. D.; Payne, M. C. *J. Phys. Chem.* **1996**, *100*, 11688-11697. (c) Bull, L. M.; Henson, N. J.; Cheetham, A. K.; Newsam, J. M.; Heyes, S. J. *J. Phys. Chem.* **1993**, *97*, 11776.
- (5) Frisch, M. J. et al. *Gaussian98*, Revision A.3; Gaussian, Inc.: Pittsburgh, PA, 1998.
- (6) (a) Izmailova, S. G.; Karentina, I. V.; Khvoshchev, S. S.; Shubaeva, M. A. *J. Colloid Interface Sci.* **1994**, *165*, 318-324. (b) Pope, C. G. *J. Chem. Soc., Faraday Trans.* **1993**, *89*, 1139-1141. (c) Gale, J. D.; Catlow, C. R. A.; Carruthers, J. R. *Chem. Phys. Lett.* **1993**, *216*, 155-159.
- (7) (a) Henson, N. J. Ph.D. thesis, Oxford University, 1996. (b) Auerbach, S. M.; Henson, N. J.; Cheetham, A. K.; Metiu, H. I. *J. Phys. Chem.* **1995**, *99*, 10600.
- (8) Kobayashi, S.; Kenmizaki, C.; Kushiya, S.; Mizuno, K. *Chem. Lett.* **1996**, 769-770.
- (9) (a) Nosé, S. *J. Chem. Phys.* **1984**, *81*, 511. (b) Hoover, W. G. *Phys. Rev. A* **1985**, *31*, 1695. (c) Martyna, G. J.; Klein, M. L.; Tuckerman, M. E. *J. Chem. Phys.* **1992**, *97*, 2635.
- (10) Andersen, H. C. *J. Chem. Phys.* **1980**, *72*, 2384-2393.
- (11) (a) Ayappa, K. G. *Rev. Chem. Eng.* **1997**, *13*, 1-69. (b) Whittington, B. I.; Milestone, N. B. *Zeolites* **1992**, *12*, 815-818.

JA017839E